THE JOURNAL OF PHYSICAL CHEMISTRY C

Article

pubs.acs.org/JPCC

Tantalum Segregation in Ta-Doped TiO_2 and the Related Impact on Charge Separation during Illumination

Leigh R. Sheppard,*[,†] Simon Hager,[‡,#] John Holik,[†] Rong Liu,[§] Sam Macartney,[∥] and Richard Wuhrer[‡]

[†]School of Computing, Engineering & Mathematics, [‡]Advanced Materials Characterisation Facility, Office of the Deputy-Vice Chancellor (Research and Development), [§]SIMS Facility, Office of the Deputy-Vice Chancellor (Research and Development), and [∥]School of Science & Health, University of Western Sydney, Locked Bag 1797, Penrith NSW 2751, Australia

Supporting Information

ABSTRACT: This investigation was aimed at identifying the influence of applied processing conditions, temperature and oxygen activity, on the segregation of Ta in Ta-doped TiO_2. Over the temperature range of 1173−1523 K, it has been observed that the tendency for Ta to segregate is greater under the application of oxidizing conditions ($p(O_2)$ = 101 kPa) than that under reducing conditions ($p(O_2)$ = $\sim 10^{-10}$ Pa). This respectively manifests as an accumulation and depletion of Ta at the surface of Ta−TiO_2 under the respective applied oxygen activities. This behavior has been interpreted in terms of the relative activities of Ta at the surface and bulk during processing. The results indicate that it is possible to substantially alter the concentration of a donor dopant at the surface of TiO_2 despite maintaining the bulk dopant loading. In so doing, a TiO_2-based homojunction is formed that can be engineered to favor charge separation, as demonstrated by preliminary surface photovoltage measurements. The optimization of this homojunction provides a promising approach for developing a novel photoelectrode material for solar-driven water splitting. This investigation has provided a fundamental basis for further investigations of compositionally graded TiO_2-based materials for improved solar harvesting.

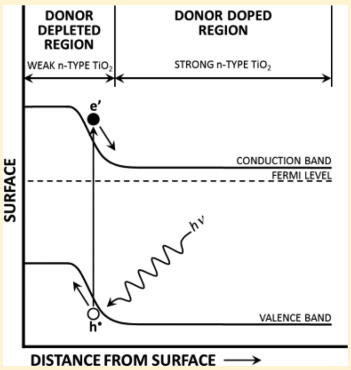

1. INTRODUCTION

The global community demands convenient access to energy, and this demand is satisfied almost exclusively by fossil fuels.[1] This dependency has created concerns over the finite availability of fossil fuels and the impact of large-scale carbon emissions on the function of the atmosphere. It is clear that alternative energy technologies are needed in order to shift away from the dependence on fossil fuels. Those technologies that are able to deliver clean and sustainable fuel are especially attractive as they most directly satisfy the challenges associated with the storage and distribution of energy.[2] Of these, solar-driven photoelectrochemical water splitting for generating hydrogen fuel is particularly attractive. This technology involves at least one photosensitive semiconductor material, which upon illumination by sunlight, facilitates the conversion of incident photons into photogenerated charge carriers. These charge carriers may then participate in redox processes that lead to the splitting of water molecules into hydrogen and oxygen.[3]

Of the various photoelectrode materials that have been studied for this application, TiO_2 has received great attention and holds great promise due to its low cost and high corrosion resistance.[3,4] Unfortunately, TiO_2 suffers from a relatively large band gap of 3−3.2 eV,[3] which limits sunlight absorption to the ultraviolet fraction of the solar spectrum.[3] Efforts to address this issue frequently involve the use of dopants to reduce the band gap and facilitate absorption of visible light.[5] However, the use of dopants has inadvertently increased recombination losses, leading to negligible performance gains.[6]

A novel way to address the apparently conflicting issues of visible light sensitivity and charge carrier recombination in doped TiO_2 is to exploit the electric fields generated by the presence of compositional gradients.[7] Such compositional gradients may be imposed through mass transport phenomena such as segregation and have been shown to promote or inhibit charge separation.[6] This approach is especially promising as an avenue through which TiO_2 may be doped to improve photosensitivity without increasing recombination losses. What is essential to this approach is being able to control the imposition of the compositional gradients, and for this, fundamental mass transport investigations are required to establish the basic behavior of various dopants in TiO_2.

In the present investigation, the segregation behavior of tantalum (Ta) in Ta-doped titanium dioxide is being studied. The aim is to establish the fundamental relationships between the segregation of Ta and the applied processing conditions, specifically temperature and oxygen activity. Of particular interest is (1) the extent to which Ta can be accumulated at the surface of Ta−TiO_2, (2) how deeply Ta segregation extends from the surface into the bulk, and (3) how sensitive Ta segregation is to changes in the applied processing conditions. With this fundamental information, Ta-doped TiO_2 may be processed in a fashion that yields a homojunction that facilitates

Received: September 28, 2014
Revised: December 2, 2014
Published: December 2, 2014

a mechanism for combining doping for improved visible light sensitivity with improved charge separation.

2. BRIEF LITERATURE REVIEW

Segregation is a mass transport process that leads to the migration of lattice defects, such as dopant species, to interfaces such as free surfaces and grain boundaries under the driving force of lattice or strain energy minimization.[8] This process, which takes place at elevated temperatures where diffusion can occur, leads to the formation of compositional variations in the vicinity of such interfaces. These compositional variations are associated with electric fields whose presence can influence the transport of electronic charge carriers such as photogenerated electrons and holes.[6] By definition, segregation is described as an equilibrium process. However, when such mass transport is taking place outside of equilibrium conditions, such as during cooling, it is referred to as nonequilibrium segregation or enrichment.[9]

Until recently,[6] solid-state processing in a manner that exploits segregation had not been investigated for engineering the functional properties of materials for solar-driven water splitting. Using surface photovoltage spectroscopy (SPS), Sheppard et al.[6] have established the experimental link between the presence of imposed compositional gradients and charge separation in Nb-doped TiO_2. It was found that processing under strongly reducing conditions leads to the depletion of Nb from the outer 15−20 nm of Nb−TiO_2 and that charge separation was noticeably improved. This was attributed to the imposition of additional band bending due to the formation of a slight homojunction. Conversely, processing under strongly oxidizing conditions resulted in the accumulation of Nb at the surface of Nb−TiO_2 and inhibited charge separation. From this investigation, it is clear that the accumulation or depletion of Nb at the surface of Nb−TiO_2 may be controlled through the appropriate application of temperature and/or oxygen activity. However, the observation of strong Nb depletion was not explained and may be unique to Nb−TiO_2. Because Nb and Ta share the same ionic radii (0.064 nm[10]) and are both donors in TiO_2, the segregation behavior of Ta in Ta-doped TiO_2 under similar processing conditions is of interest.

Ta-doped TiO_2 has received some recent attention as a material for solar energy conversion[11−15] and gas sensing.[16] Notable performance outcomes include a photovoltaic efficiency of 8.18%[11] and a high open-circuit voltage of 0.87 V when applied to dye-sensitized solar cells.[13] In all applications, interfacial charge transfer is playing a key role in determining applied performance. However, there is a general lack of consideration for how the loading of Ta at the surface may or may not differ from that of the bulk due to the occurrence of mass transport processes during material synthesis. Hence, knowledge of the tendency for Ta to segregate or enrich the surface of TiO_2 in response to various applied processing conditions may prove important for improving the performance of Ta-based materials in these applications.

To date, the only known investigation of Ta segregation in Ta−TiO_2 has been reported by Sheppard et al.[17] This investigation considered only a single dopant concentration (1.0 at. % Ta) and observed that the accumulation of Ta at the surface of Ta−TiO_2 was favored by the application of oxidizing conditions. Under strongly reducing conditions, Ta was observed to become depleted from the surface when the applied temperature exceeded 1348 K. The reason for this behavior was not clearly identified; however, it was suggested that Ta may be evaporating from the surface and into the gas phase. Very similar behavior to this was also observed in Nb-doped TiO_2.[8] However, in the case of Nb−TiO_2, depletion was observed under all studied annealing temperatures. Given the similarities between Nb and Ta, this similar behavior is not unexpected. Additional investigations on Nb segregation have also been reported,[18−22] but direct comparisons are challenging due to the absence of kinetic information to confirm the presence of equilibrium and, thereby, the ease of reproducibility. Nonetheless, all of these reports confirm that the segregation of Nb in Nb-doped TiO_2 is highly sensitive to the applied processing conditions. This is promising for imposing compositional gradients within TiO_2 in a controlled manner.

3. EXPERIMENTAL PROCEDURE

Sample Preparation. Samples of Ta-doped TiO_2 were prepared using the sol−gel technique and involved high-purity titanium butoxide (Sigma-Aldrich, Australia) and Ta butoxide (Sigma-Aldrich, Australia) as precursors. Initially, a titanium precursor solution of titanium butoxide and isopropanol (Sigma-Aldrich, Australia) was prepared to a molar ratio of 1:6.4, respectively, and stirred at room temperature for 2 h. Independently, a 1.27 mol L^{-1} solution of Ta butoxide in isopropanol was prepared for the inclusion of the Ta dopant. From this solution, a volume was added in a dropwise fashion to the titanium precursor solution to achieve nominal Ta dopant loadings of 0.25, 0.50, 1.0, and 2.5 atom % Ta. Stirring was maintained throughout and continued for a further 2 h afterward without heating. After this time, two drops of hydrochloric acid (Sigma-Aldrich, Australia) were added. After a further 2 h of stirring, 284 mL of a 5:4 molar ratio solution of isopropanol and distilled water were dropwise added to initiate precipitation of Ta-doped Ti species. This final solution was warmed to 80 °C and stirred overnight.

The resulting precipitate was subsequently ground in an agate mortar and pestle before being calcined in a Pt-lined alumina boat and inserted into a horizontal tube furnace for 3 h at 450 °C in air. The heating ramp was 1 °C/min, and the cooling ramp was 5 °C/min. From the as-calcined batch of powder, a number of pellets were prepared by uniaxial pressing to ∼40 MPa followed by cold isostatic pressing to 400 MPa. These pellets were again placed on a Pt-lined alumina boat and sintered at 1673 K for 10 h in air in a horizontal tube furnace with a high-purity alumina tube. After this densification step, one face of each pellet was polished to a high mirror finish that began with a 65 μm grinding pad and proceeded in a stepwise fashion through finer pads to conclude with a 1 μm lapping pad. Once the final polishing step had been completed, the pellets were cut into bricks of ∼3 mm thickness, 2.5 mm width, and 5−10 mm length using a precision cutoff saw (Struers Accutom, Struers, Australia).

After this preparation, individual samples were annealed in a horizontal tube furnace (on Pt-lined alumina boats as previous) at different temperatures, 1173, 1348, and 1523 K for 50 h, and in a gas phase of either high or low oxygen activity. High oxygen activity, hereafter referred to as "oxidizing" was achieved through the use of 99.9% pure oxygen gas (Coregas, Australia) flowing (100 sccm) through the alumina process tube during annealing. As such, the oxygen partial pressure was 101 kPa. Low oxygen activity, hereafter referred to as "reducing", was achieved through the use of 1%H_2/99%Ar gas (Coregas), which was saturated with water vapor by bubbling through

dx.doi.org/10.1021/jp509806h | J. Phys. Chem. C 2015, 119, 392−400

milli-q water at 2.5 °C, and then flowed (100 sccm) through the process tube during annealing. In this case, the oxygen partial pressure was in the vicinity of 10^{-10} Pa but varied marginally with changes in temperature due to H_2/H_2O equilibria.

Preliminary Characterization. Some preliminary characterization was undertaken to confirm basic sample details and to confirm the success of the sample preparation process. This characterization involved imaging with scanning electron microscopy (SEM) and phase confirmation using X-ray diffraction (XRD). SEM was performed using a JEOL 7001F field emission gun SEM (Jeol, Japan). The accelerating voltage was 15 kV, and the working distance set to 10 mm. In order to see a clear microstructure, an as-polished sample was thermally etched in air at 1250° for 15 min prior to imaging. XRD was performed on a Bruker D8 Advance diffractometer fitted with a Lynxeye detector (Bruker, Germany), with Ni-filtered Cu Kα radiation of 1.54056 nm wavelength. The scan was collected from 20 to 90° 2-theta, with 0.02° steps and a 1 s/step acquisition time.

X-ray Photoelectron Spectroscopy. The surface composition of all specimens was determined using a Thermo Scientific ESCALAB 250Xi instrument (Thermo Scientific, U.S.A.). The X-ray source consisted of monochromatic Al Kα X-rays of 1486.68 eV energy and an operating power of 164 W. The photoelectron takeoff angle was 90°, and the pass energy was 100 eV for survey scans and 20 eV for narrow scans. The spot size was 500 μm in diameter, and the base vacuum of the analysis chamber was 2×10^{-7} Pa. All binding energies were calibrated to the C 1s photoelectron peak at 284.8 eV, which corresponds to adventitious surface hydrocarbon contamination. The obtained spectra were resolved into Gaussian–Lorentzian components after background subtraction using the Shirley fitting routine.[23] The concentration of all detected species was determined using Avantage software (Thermo Scientific, U.K.).

Secondary Ion Mass Spectrometry. Secondary ion mass spectrometry (SIMS) was used to determine depth profiles of ^{181}Ta in all specimens by using a Cameca IMS 5fE7 SIMS instrument (Cameca, France). A primary ion beam of O_2^+ with an impact energy of 7.5 keV and beam current of 10 nA was employed to raster a 150 μm × 150 μm region of the surface, with an analysis area of 8 μm diameter in the center of the rastered area in order to avoid crater effects. The samples were gold coated to prevent sample charging during analysis. The secondary ions included $^{181}Ta^+$, $^{48}Ti^+$, $^{48}Ti^{16}O^+$, and $^{197}Au^+$. To avoid artifacts associated with the damage caused by cutting the specimens, analysis was always undertaken centrally on the samples surface. The sputter rate was determined by sputtering a particularly deep analysis crater on an epi-polished TiO_2 crystal (SurfaceNet, Germany) and assessing its depth using a KLA Tencor Alpha-Step IQ profilometer (KLA-Tencor, U.S.A.). The average sputter rate was thus determined to be 0.0344 nm/s.

4. RESULTS

Preliminary Characterization. After sintering, XRD traces and SEM micrographs were obtained from a specimen of each composition to confirm preliminary details. After sintering at 1673 K, all specimens attained the rutile TiO_2 structure, and no second phases were detected. This indicates that the applied Ta doping levels were within the limits of solubility. From imaging with SEM, the grain size distribution observed in each specimen was not large, with the majority of grains ranging from 5 to 10 μm in diameter. The extent of porosity was consistent with bulk density ranging from 85 to 90% as determined using the Archimedes method.

XRD analysis and SEM imaging were repeated on all samples after the various annealing treatments to identify any changes to structure or morphology. The obtained XRD traces confirmed the sole presence of rutile TiO_2 and failed to detect any second phases. SEM imaging revealed that some minor grain growth resulted from the annealing treatments, especially at 1523 K. At this temperature, the typical grain size was approximately 10 μm. Grain boundary faceting was observed to be favored by Ta dopant loading, increasing temperature and annealing under oxidizing conditions.

X-ray Photoelectron Spectroscopy Results. In order to determine the surface concentration of Ta, $[Ta]_{Surf}$, XPS has been employed to analyze the surface composition of all specimens after annealing. A typical survey spectrum is displayed as Figure 1. As seen, this spectrum identifies

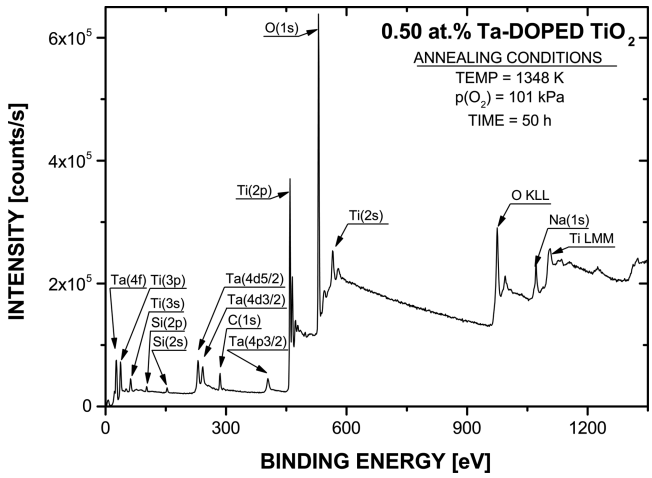

Figure 1. X-ray photoelectron spectroscopy survey scan obtained from the surface of 0.50 atom % Ta-doped TiO_2 that has been annealed in $p(O_2)$ = 101 kPa at 1348 K for 50 h.

photoelectron peaks for the major elements of interest, Ti $2p_{3/2}$ (459 eV), O 1s (530 eV), Ta 4f (27 eV), and C 1s (285 eV), as well as photoelectron peaks for minor impurities, Na and Si, and alternative electron orbitals for Ti and Ta. Narrow scans were obtained for each of the key elements of interest and used to determine $[Ta]_{Surf}$. A typical set of narrow scans is displayed as Figure 2. These were obtained from 0.50 atom % Ta–TiO_2 annealed at 1348 K in oxidizing conditions. These higher-resolution spectra reveal additional photoelectron peaks to those already identified from the survey spectra. Ta 4f was found to consist of two peaks, $4f_{7/2}$ and $4f_{5/2}$, with binding energies of 26.2 and 28.1 eV, respectively. These photoelectron peaks are consistent with those found previously by Sheppard et al.[17] and are consistent with the presence of Ta^{5+}.[15] Titanium was also found to consist of two photoelectron peaks, Ti $2p_{3/2}$ A and Ti $2p_{3/2}$ B, at 459.1 and 457.4 eV, respectively, which is consistent with literature reports.[24,25] These respectively correspond to the 4+ and 3+ valence states of Ti.[24] Their relative intensity in this particular specimen indicates the predominance of the 4+ state, which is consistent with the application of oxidizing conditions. Oxygen has been observed to consist of several photoelectron peaks, O 1s A (530.3 eV), O

dx.doi.org/10.1021/jp509806h | J. Phys. Chem. C 2015, 119, 392–400

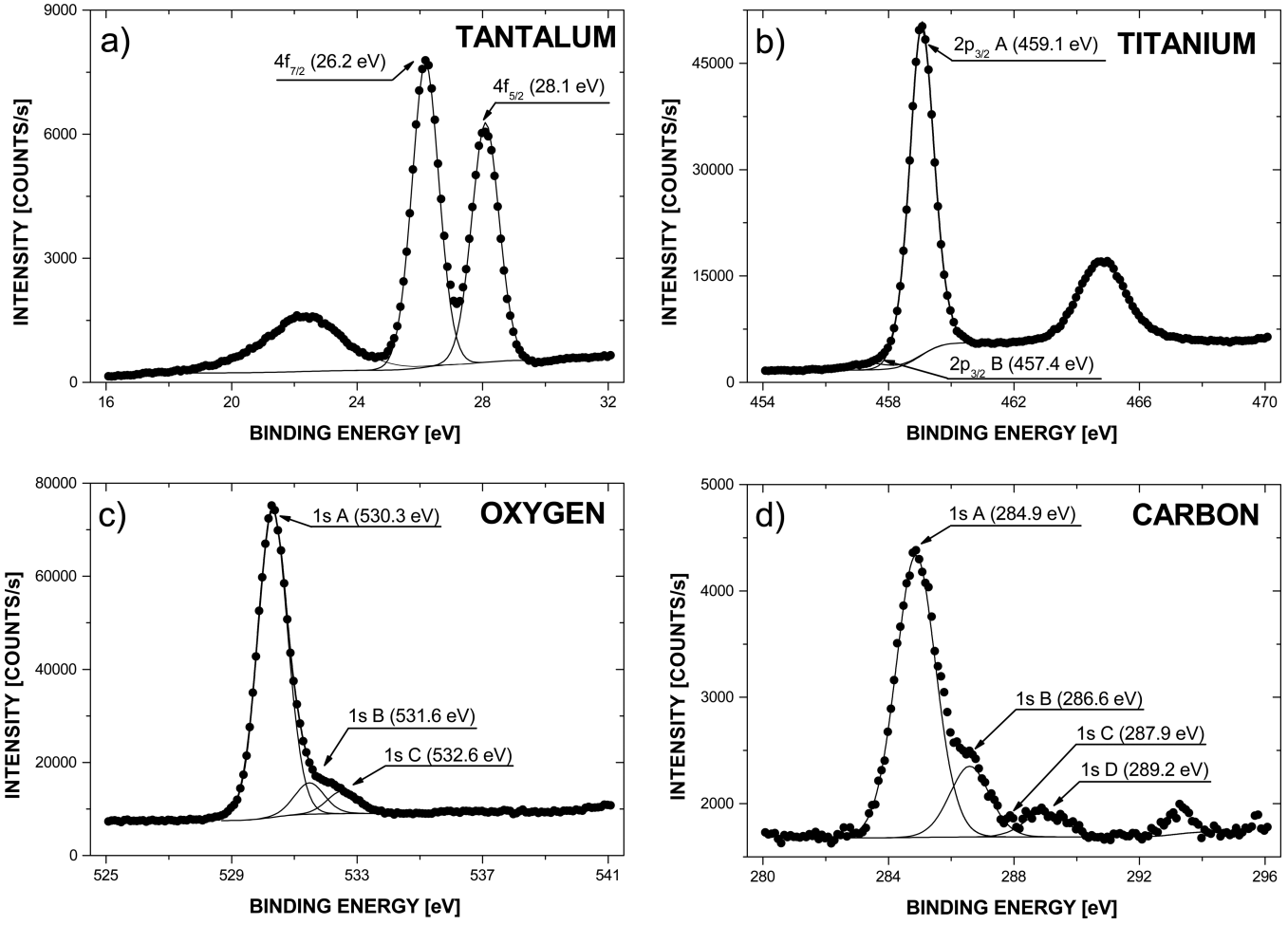

Figure 2. X-ray photoelectron spectroscopy narrow scan spectra for (a) Tantalum, (b) titanium, (c) oxygen, and (d) carbon photoelectron peaks obtained from the surface of 0.50 atom % Ta-doped TiO_2 that has been annealed in $p(O_2)$ = 101 kPa at 1348 K for 50 h.

1s B (531.6 eV), and O 1s C (532.6 eV). According to the literature, these respectively correspond to lattice oxygen (530.1 eV[8]) and surface hydroxides at binding energies of 531.6 and 532.6 eV,[26] respectively. The presence of adventitious hydrocarbons is evident from the photoelectron peaks observed for carbon.[24]

From the XPS analysis, $[Ta]_{Surf}$ has been determined for each dopant loading and applied annealing condition. This data is summarized in Figure 3 and displays several general trends. Aside from the behavior observed at 1173 K in oxidizing conditions, decreasing temperature has resulted in an increase in $[Ta]_{Surf}$ under both oxidizing and reducing conditions. Similarly, increasing the bulk concentration of Ta, $[Ta]_{Bulk}$, has also resulted in an increase in $[Ta]_{Surf}$ in all conditions except oxidizing at 1173 K. A comparison of the application of oxidizing and reducing conditions as a function of $[Ta]_{Bulk}$ at different temperatures is displayed in Figure 4. As seen, the application of oxidizing conditions yields greater $[Ta]_{Surf}$ than reducing conditions. At 1173 K, this situation holds for $[Ta]_{Bulk}$ of 1.00 atom % Ta and under but is strongly trending toward $[Ta]_{Surf}$, favoring the application of reducing conditions.

SIMS Results. In order to determine the Ta segregation profiles that have been imposed in each Ta–TiO_2 sample, SIMS analysis has been utilized. Elemental yields for ^{48}Ti, $^{48}Ti^{16}O$, ^{197}Au, and ^{181}Ta were obtained, which, respectively, relate to the two matrix elements, the gold coating, and the dopant species. A sharp initial rise in yield intensities for each element was also observed due to the establishment of steady-

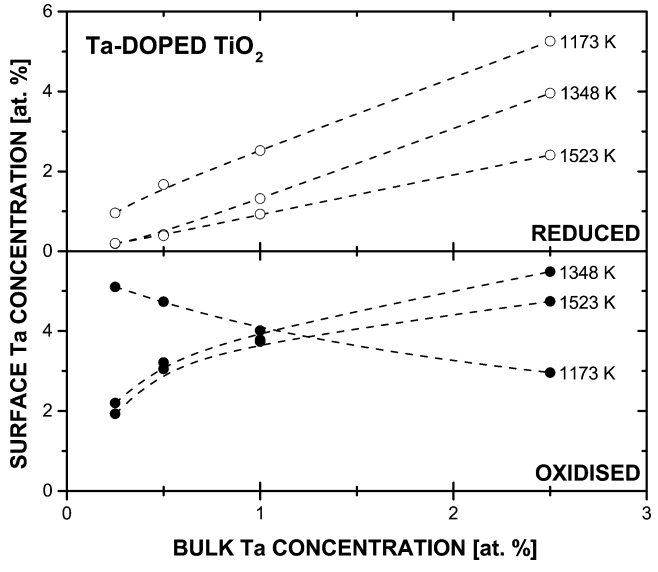

Figure 3. Summary of the effect of temperature and oxygen activity on the surface concentration of Ta in Ta-doped TiO_2 at each bulk Ta dopant concentration. Note that "reduced" refers to $p(O_2)$ = $\sim 10^{-10}$ Pa, and "oxidized" refers to $p(O_2)$ = 101 kPa.

dx.doi.org/10.1021/jp509806h | J. Phys. Chem. C 2015, 119, 392–400

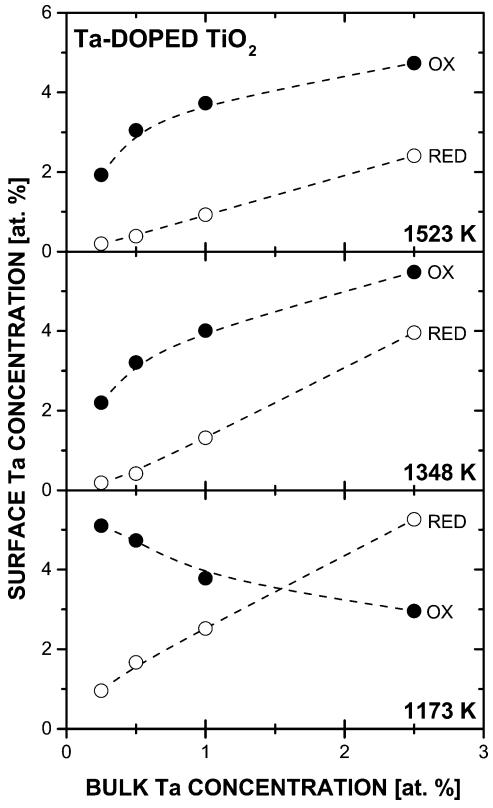

Figure 4. Summary of the effect of temperature and oxygen activity on the surface concentration of Ta in Ta-doped TiO_2 at each bulk Ta dopant concentration. Note that "red" refers to $p(O_2)$ = ~10^{-10} Pa, and "ox" refers to $p(O_2)$ = 101 kPa.

state sputtering upon commencing SIMS analysis. This creates uncertainty concerning the composition of the samples surface and is further complicated by the presence of a Au coating. This is an unavoidable aspect of SIMS analysis and requires that the initially acquired data be discarded. This corresponds to approximately the first 100 s of analysis, which has consequently been removed from all SIMS data.

In order to extract reliable concentration information from SIMS data, accurate and specifically prepared reference specimens are required. However, in the absence of such reference specimens, it is possible to consider the concentration of Ta using the following expression[8]

$$\frac{I(^{181}\mathrm{Ta})}{I(^{48}\mathrm{Ti})} \propto C_{\mathrm{Ta}} \tag{1}$$

where $I(^{181}\mathrm{Ta})$ and $I(^{48}\mathrm{Ti})$ represent the yield intensity of ^{181}Ta and ^{48}Ti, respectively, and C_{Ta} represents the concentration of Ta, which varies linearly with the actual concentration of Ta. In Figure 5, SIMS depth profiles have been expressed as the ratio of the yield intensities of ^{181}Ta and ^{48}Ti in order to reflect relative changes in the Ta segregation profiles with depth.

The effect of applied oxygen activity at 1348 K is illustrated in Figure 5a and b. As seen, under oxidizing conditions (Figure 5a), Ta is observed to enrich the surface of Ta−TiO_2 for Ta dopant concentrations up to and including 1.00 atom %. However, for 2.50 atom % Ta−TiO_2, the Ta concentration profile shows some evidence of Ta depletion at the immediate surface, while Ta enrichment is evident from ~5 nm below the surface and deeper. Under these processing conditions, the depth of the segregation-affected region is ~30 nm. From

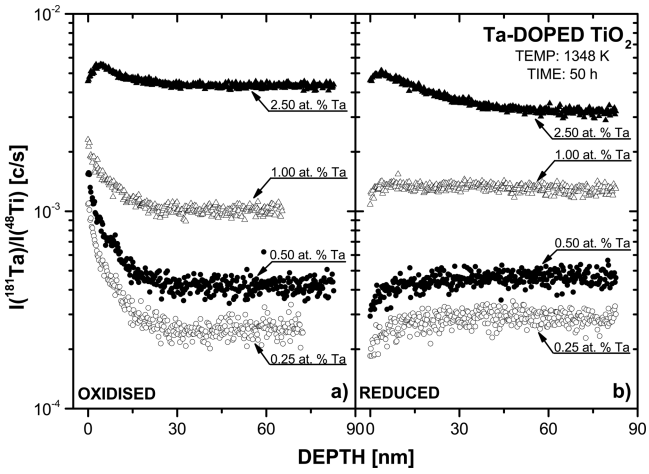

Figure 5. Summary of processed SIMS depth profiles for all Ta-doped TiO_2 compositions annealed at 1348 K for 50 h. Note that "reduced" refers to $p(O_2)$ = ~10^{-10} Pa, and "oxidized" refers to $p(O_2)$ = 101 kPa.

Figure 5b, the application of reducing conditions has largely had the opposite effect to oxidizing conditions and resulted in the depletion of Ta from the surface of Ta−TiO_2 for Ta dopant loadings up to and including 1.00 atom %. However, for 2.50 atom % Ta, a mix of Ta enrichment and depletion is once again observed. Under these processing conditions, the depth of the segregation-affected region is ~15 nm.

In order to compare the relative extent of Ta segregation between different specimens, it is convenient to consider the enrichment factor, f, which is defined as the ratio of Ta surface concentration to Ta bulk concentration as expressed by eq 2

$$f = \frac{[\mathrm{Ta}]_{\mathrm{Surf}}}{[\mathrm{Ta}]_{\mathrm{Bulk}}} \tag{2}$$

The enrichment factor has been thus calculated for all specimens and is summarized in Figure 6. As seen in this figure, Ta segregation is favored by the application of oxidizing conditions at all temperatures and Ta dopant levels. The only exception is at 1173 K for 2.50 atom % Ta−TiO_2, where Ta enrichment under reducing conditions is slightly greater than that under oxidizing conditions. Given the range of f for all other Ta dopant loadings, this result is likely within the uncertainty of the experiment, and it can be considered that at 2.50 atom % Ta, f is independent of the applied oxygen activity for 1173 K and perhaps also for 1348 and 1523 K.

What is also evident from Figure 6 is the sensitivity of the enrichment factor (f) to applied temperature. Under the application of oxidizing conditions, the enrichment factor is observed to decrease noticeably from 1173 to 1348 K but is only slightly reduced upon increasing the temperature further to 1523 K. Similar behavior is observed when applying reducing conditions. This suggests that temperature affects segregation in largely the same way, independently of the applied oxygen activity.

5. DISCUSSION

From the results obtained for this investigation, it is clear that temperature, oxygen activity, and Ta doping level all have an important impact on both the extent of Ta surface segregation and its nature in terms of accumulation or depletion at the surface. In order to explain the observed behavior, the results must be divided into general categories that appear to represent

dx.doi.org/10.1021/jp509806h | J. Phys. Chem. C 2015, 119, 392−400

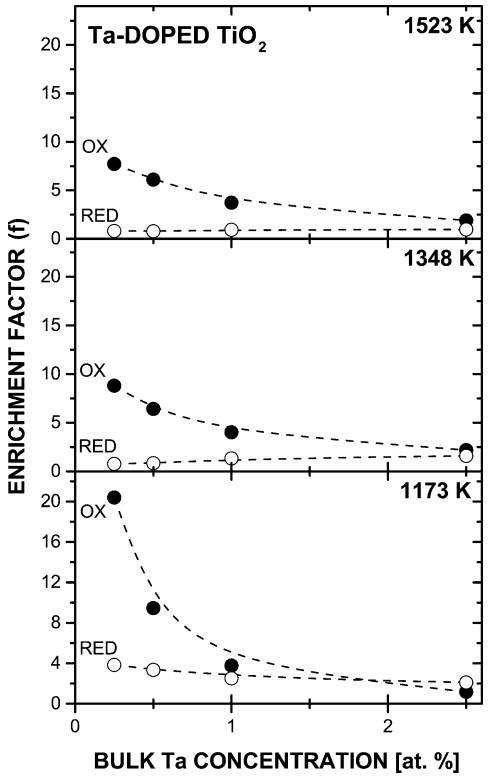

Figure 6. Summary of the determined enrichment factor for each bulk Ta concentration. Note that "red" refers to $p(O_2) = \sim 10^{-10}$ Pa, and "ox" refers to $p(O_2) = 101$ kPa.

specific regimes of behavior. These correspond to the applied processing temperature, and the results obtained at 1173 K should be considered separately from those obtained at 1348 and 1523 K.

At 1348 and 1523 K, altering the applied oxygen activity has had a clear impact on the tendency for Ta to segregate. This is most clearly illustrated in Figure 4, where, in terms of $[Ta]_{Surf}$, the application of oxidizing condition has consistently yielded Ta accumulation at the surface. In contrast, the application of reducing conditions has resulted in either the depletion of Ta from the surface or Ta accumulation at a reduced extent.

This behavior can be considered in terms of the activity of Ta at the surface, a_{Ta}^{Surf}, and the activity of Ta in the bulk, a_{Ta}^{Bulk}. As schematically illustrated in Figure 7, initially ($t = 0$), the concentrations of $[Ta]_{Surf}$ and $[Ta]_{Bulk}$ would be equal due to

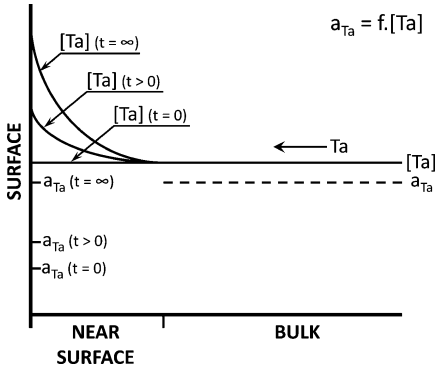

Figure 7. Schematic illustration of the behavior of the surface and bulk activity of Ta as time, t, proceeds.

the sample preparation procedure (polished surface). However, a_{Ta}^{Surf} and a_{Ta}^{Bulk} would be quite different. Implied from the obtained results for those specimens that display Ta surface accumulation, initially, a_{Ta}^{Surf} must be significantly less than a_{Ta}^{Bulk}. This disparity in the activity of Ta would create a driving force for the migration of Ta toward the surface and increase $[Ta]_{Surf}$ according to the following relationship between concentration, c, activity coefficient, f, and activity, a[8]

$$a = f \cdot c \tag{3}$$

It is pointed out that f in this case is not to be confused with the enrichment factor (see eq 2). At equilibrium ($t = \infty$), the activity of the surface and bulk would be equal, and therefore, $[Ta]_{Surf}$ would cease to increase. The observation of Ta depletion can be accounted for in a similar way to Ta accumulation, except that initially (at $t = 0$), a_{Ta}^{Surf} must be greater than a_{Ta}^{Bulk}. Consequently, $[Ta]_{Surf}$ decreases as a_{Ta}^{Surf} approaches a_{Ta}^{Bulk}.

Through doping, $[Ta]_{Bulk}$ has been increased. This will lead to an increase in a_{Ta}^{Bulk}, but this increase in activity appears to be more significant at lower doping levels than at high. Consequently, the change in driving force for Ta migration to the surface is reduced as $[Ta]_{Bulk}$ is increased. This is most clearly reflected by the behavior of the enrichment factor displayed in Figure 6.

At equilibrium, a_{Ta}^{Surf} must also be equal to the activity of Ta in the gas phase, a_{Ta}^{Gas}. However, in the present experiment, the use of a flowing gas phase will preclude true gas−solid equilibrium. Nevertheless, a_{Ta}^{Gas} will be especially low irrespective of the applied gas mixture or temperature due to this feature. Consequently, it can be expected that under the application of oxidizing conditions, where a_{Ta}^{Surf} assumes lower levels than when reducing conditions are applied, the tendency for Ta evaporation will be relatively less. This can account for the behavior illustrated in Figure 5b where the depletion of Ta appears to be limited to the very close proximity of the absolute surface (<10 nm).

In principle, this lack of equilibrium at the surface means that the entire system is not at equilibrium and that the obtained results should be strictly considered as enrichment behavior rather that segregation behavior. However, in the absence of kinetic data, such a strict interpretation is limiting. It has been shown from electrical conductivity measurements of Nb-doped TiO_2 that equilibrium under reducing conditions may be attained within a few hours, and such measurements continue to remain stable for many hours thereafter.[27] This attests to the stability of the bulk, despite a clearly active surface, as shown by Sheppard et al.[8] It is thus considered likely that the kinetics of Nb evaporation (and similarly Ta evaporation) are slow and fail to noticeably disturb the mass transport processes taking place within the bulk and near-surface regions. Hence, at 1348 and 1523 K, the observed behavior of Ta may be considered to be indicative of Ta segregation that is close to equilibrium, if not entirely reaching equilibrium.

In view of the above consideration of equilibrium, the results obtained at 1173 K must be considered differently. As seen in Figure 3, under oxidizing conditions, the trend for $[Ta]_{Surf}$ with increasing $[Ta]_{Bulk}$ is entirely different at 1173 K to what is observed at 1348 and 1523 K. In contrast, under reducing conditions, the behavior at 1173 K is in line with observations at 1348 and 1523 K.

Under oxidizing conditions, the incorporation of Ta into TiO_2 can be described using the following chemical equilibria

dx.doi.org/10.1021/jp509806h | J. Phys. Chem. C 2015, 119, 392−400

and associated simplified electroneutrality condition, utilizing Kröger–Vink notation[28]

$$2Ta_2O_{5(s)} \leftrightarrow 4Ta_{Ti}^{\bullet} + V_{Ti}^{''''} + 10O_O^x \quad (4)$$

$$[Ta_{Ti}^{\bullet}] = 4[V_{Ti}^{''''}] \quad (5)$$

where $Ta_{Ti}^{\bullet}$ represents a substitutional Ta^{5+} ion in a regular Ti lattice site, $V_{Ti}^{''''}$ represents a quadruply charged titanium vacancy, and O_O^x represents a regular neutral oxygen species on an oxygen site. Square brackets, e′, and n have their conventional meanings. In this case, which describes a particular regime where the defect disorder is simplified to be limited to majority species for convenience, the incorporation of Ta is charge compensated by ionic species, titanium vacancies.

Under reducing conditions, the incorporation of Ta into TiO_2 can be similarly expressed as

$$2Ta_2O_{5(s)} \leftrightarrow 4Ta_{Ti}^{\bullet} + 8O_O^x + 4e' + O_{2(g)} \quad (6)$$

$$[Ta_{Ti}^{\bullet}] = n \quad (7)$$

where incorporated Ta is charge compensated by electrons.

The mode of charge compensation, ionic versus electronic, has an important consequence for the migration of Ta throughout the TiO_2 lattice. Under oxidizing conditions, the diffusion of Ta will be accompanied by the diffusion of Ti vacancies, which, according to Nowotny et al.,[29] is especially slow. In contrast, under reducing conditions, the diffusion of Ta would be accompanied by electrons whose mobility is relatively high. Hence, the anomalous Ta segregation behavior observed at 1173 K for oxidizing conditions may be attributed to poor Ta migration kinetics and as such cannot be considered representative of equilibrium. Verification of this would require an investigation of segregation kinetics, which is beyond the scope of the present investigation but is clearly needed for a more complete understanding of this system.

6. IMPLICATIONS FOR SOLAR-DRIVEN WATER SPLITTING

The present investigation is part of an ongoing research effort to develop an advanced form of TiO_2 that may be utilized as a photoelectrode for solar-driven water splitting. In this application, effective charge separation has been identified as a barrier to achieving high performance.[6] Recently, it has been suggested that the formation of a homojounction consisting of strongly n-type bulk with a weakly n-type (or potentially p-type) surface and near-surface region would favor strong charge separation (schematically represented in Figure 8). Ta doping satisfies the requirement for a strongly n-type bulk, and from the results obtained in the present investigation, promoting the depletion of Ta from the surface and near-surface region by processing in reducing conditions could be expected to yield a promising homojunction.

In order to test this hypothesis, preliminary measurements of charge separation have been obtained using SPS (experimental details are available as Supporting Information) for two specimens selected for their high degree of Ta surface enrichment and surface depletion (see Figure 9a). By measuring changes in the surface electrical potential of a material due to the migration of photoelectrons either toward or away from the surface during illumination,[6] this technique provides a means for assessing the abilities of a material to

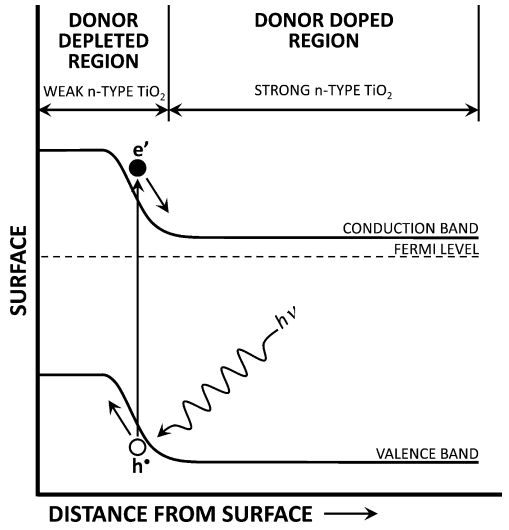

Figure 8. Schematic illustration of a proposed TiO_2-based homojunction that consists of donor-depleted and donor-doped TiO_2 and exhibits enhanced charge separation properties.

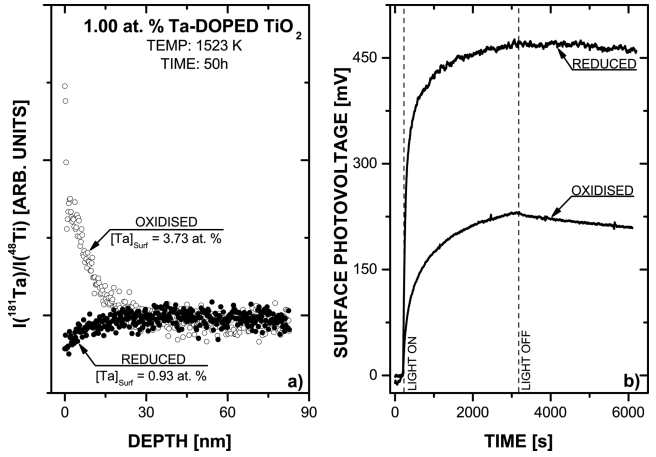

Figure 9. (a) SIMS depth profiles for 1.00 atom % Ta Ta-doped TiO_2 processed at 1523 K for 50 h in oxidized ($p(O_2)$ = 101 kPa) and reduced conditions ($p(O_2)$ = $\sim 10^{-10}$ Pa). (b) Surface photovoltage generated during monochromatic illumination (310 nm) of the two Ta-doped TiO_2 specimens represented in (a).

separate photogenerated charge carriers. As seen in Figure 9b, the surface photovoltage developed during monochromatic illumination (310 nm) of these two samples differs markedly. This corresponds to clear differences in the distribution of Ta within the surface and near-surface region due to applied processing (see Figure 9a) and clearly indicates that charge separation is favored when the surface is depleted in Ta. While still preliminary in nature, this result supports the proposed role of TiO_2-based homojunctions for improved solar energy conversion.

The current results also indicate that the depth of the Ta-depleted region is very shallow (15 nm or less), and it would need to be made much deeper (500–1000 nm) if visible photons were to be strongly absorbed within the influence of the imposed electric field. This may prove difficult if processing is restricted to the bounds of equilibrium.

On the other hand, nonequilibrium processing may provide a way forward. The fabrication of a multilayer photoelectrode material consisting of Ta–TiO_2 layers of incrementally altered

dx.doi.org/10.1021/jp509806h | J. Phys. Chem. C 2015, 119, 392–400

Ta loading would provide a means for simultaneously controlling both the extent of $[Ta]_{Surf}$ depletion *and* the depth of the near-surface region affected by the imposed compositional variation. This route is attractive by providing the means for tuning the compositional profile to maximize both the absorption of visible light and charge separation. On the basis of the segregation behavior observed in this report, such control would be unavailable via equilibrium processing routes.

7. CONCLUSIONS

The present investigation has considered the impact of different applied processing conditions on the surface segregation of Ta in Ta-doped TiO_2. From these results, it is clear that Ta can be enriched or depleted in the surface and near-surface region depending mostly on the applied oxygen activity but also on the temperature and the bulk Ta doping level. Reducing conditions appear to increase the activity of Ta at the surface, leading to Ta depletion, whereas the application of oxidizing conditions lowers the activity of Ta at the surface, leading to Ta enrichment. Over the studied temperature range, the kinetics of Ta diffusion appear to be relatively swift under reduced conditions. However, the transport kinetics of Ta appear to be slower under the application of oxidizing conditions, and at 1173 K, the observed behavior is considered reflective of enrichment rather than segregation. These differences in transport kinetics are attributed to the ionic compensation of Ta incorporation at high oxygen activity and electronic compensation at low oxygen activity. Preliminary SPS measurements indicate that depleting the surface and near-surface region of Ta is considerably more favorable for charge separation than Ta enrichment. This supports the hypothesis of a TiO_2-based homojunction for improved water splitting. The obtained results provide important processing insights into the fabrication of TiO_2-based photoelectrode materials for solar energy harvesting.

■ ASSOCIATED CONTENT

Supporting Information

Experimental details for the obtaining of surface photovoltage measurements. This material is available free of charge via the Internet at http://pubs.acs.org.

■ AUTHOR INFORMATION

Corresponding Author

*E-mail: L.Sheppard@uws.edu.au. Tel: +61 2 4570 1745. Fax: +61 2 4570 1369.

Present Address

[#]Electron Microscopy Unit, Mark Wainwright Analytical Centre, University of New South Wales, Sydney, NSW 2052, Australia.

Author Contributions

The manuscript was written through contributions of all authors. All authors have given approval to the final version of the manuscript. These authors contributed equally.

Notes

The authors declare no competing financial interest.

■ ACKNOWLEDGMENTS

This work was supported by the Australian Research Council's Discovery Project funding scheme (Project Number DP0987084). Also acknowledged is the support of Dr. Bin Gong at the University of New South Wales Mark Wainwright Analytical Centre for performing the XPS analysis in this investigation. The contribution of SPS data and discussion by Dr. Thomas Dittrich of the Institute for Heterogeneous Materials Systems at the Helmholtz-Centre for Materials and Energy Berlin is also sincerely acknowledged. The authors also warmly acknowledge the staff of the UWS Advanced Materials Characterisation Facility for their assistance with the collection of XRD and SEM data and follow up discussions.

■ REFERENCES

(1) Ball, M.; Wietschel, M. The Future of Hydrogen — Opportunities and Challenges. *Int. J. Hydrogen Energy* **2009**, *34*, 615−627.

(2) Nowotny, J.; Sorrell, C. C.; Sheppard, L. R.; Bak, T. Solar-Hydrogen: Environmentally Safe Fuel for the Future. *Int. J. Hydrogen Energy* **2005**, *30*, 521−544.

(3) Sheppard, L. R.; Nowotny, J. Materials for Photoelectrochemical Energy Conversion. *Adv. Appl. Ceram.* **2007**, *106*, 9−20.

(4) Fujishima, A.; Honda, K. Electrochemical Photolysis of Water at a Semiconductor Electrode. *Nature* **1972**, *238*, 37−38.

(5) Nowotny, J.; Bak, T.; Nowotny, M. K.; Sheppard, L. R. Titanium Dioxide for Solar Hydrogen I. Functional Properties. *Int. J. Hydrogen Energy* **2007**, *32*, 2609−2629.

(6) Sheppard, L. R.; Dittrich, T.; Nowotny, M. K. The Impact of Niobium Surface Segregation on Charge Separation in Niobium-Doped Titanium Dioxide. *J. Phys. Chem. C* **2012**, *116*, 20923−20929.

(7) Nowotny, M. K.; Sheppard, L. R.; Bak, T.; Nowotny, J. Defect Chemistry of Titanium Dioxide. Application of Defect Engineering in Processing of TiO_2-Based Photocatalysts. *J. Phys. Chem. C* **2008**, *112*, 5275−5300.

(8) Sheppard, L. R. Niobium Surface Segregation in Polycrystalline Niobium-Doped Titanium Dioxide. *J. Phys. Chem. C* **2013**, *117*, 3407−3413.

(9) Harries, D. R.; Marwick, A. D. Non-equilibrium Segregation in Metals and Alloys. *Philos. Trans. R. Soc. London, Ser. A* **1980**, *295*, 197−207.

(10) Lide, D. R. *CRC Handbook of Chemistry and Physics*, 84th ed.; CRC Press: Boca Raton, FL, 2003.

(11) Liu, J.; Yang, H.; Tan, W.; Zhou, X.; Lin, Y. Photovoltaic Performance Improvement of Dye-Sensitized Solar Cells Based on Tantalum-Doped TiO_2 Thin Films. *Electrochim. Acta* **2010**, *56*, 396−400.

(12) Niishiro, R.; Kato, H.; Kudo, A. Nickel and Either Tantalum or Niobium-Codoped TiO_2 and $SrTiO_3$ Photocatalysts with Visible-Light Response for H_2 or O_2 Evolution From Aqueous Solutions. *Phys. Chem. Chem. Phys.* **2005**, *7*, 2241−2245.

(13) Feng, X.; Shankar, K.; Paulose, M.; Grimes, C. A. Tantalum-Doped Titanium Dioxide Nanowire Arrays for Dye-Sensitized Solar Cells with High Open-Circuit Voltage. *Angew. Chem., Int. Ed.* **2009**, *48*, 8095−8098.

(14) Znad, H.; Ang, M. H.; Tade, M. O. Ta/TiO_2- and Nb/TiO_2-Mixed Oxides as Efficient Solar Photocatalysts: Preparation, Characterisation, and Photocatalytic Activity. *Int. J. Photoenergy* **2012**, No. Art. ID548158.

(15) Obata, K.; Irie, H.; Hashimoto, K. Enhanced Photocatalytic Activities of Ta, N Co-doped TiO_2 Thin Films under Visible Light. *Chem. Phys.* **2007**, *339*, 124−132.

(16) Bonini, N.; Carotta, M. C.; Chiorino, A.; Guidi, V.; Malagu, C.; Martinelli, G.; Paglialonga, L.; Sacerdoti, M. Doping of a Nano-structured Titania Thick Film: Structural and Electrical Investigations. *Sens. Actuators, B* **2000**, *68*, 274−280.

(17) Sheppard, L. R.; Holik, J.; Liu, R.; Macartney, S.; Wuhrer, R. Tantalum Enrichment in Tantalum-Doped Titanium Dioxide. *J. Am. Ceram. Soc.* **2014**, DOI: 10.1111/jace13201.

(18) Sheppard, L. R.; Atanacio, A.; Bak, T.; Nowotny, J.; Prince, K. E. Effect of Niobium Segregation on the Surface Properties of Titanium Dioxide. *Proc. SPIE* **2006**, *6340*, 634015.

(19) Nakajima, T.; Sheppard, L. R.; Prince, K. E.; Nowotny, J.; Ogawa, T. Niobium Segregation in TiO_2. *Adv. Appl. Ceram.* **2007**, *106*, 82−88.
(20) Ruiz, A. M.; Dezanneau, G.; Arbiol, J.; Cornet, A.; Morante, J. R. Insights into the Structural and Chemical Modifications of Nb Additive on TiO_2 Nanoparticles. *Chem. Mater.* **2004**, *16*, 862−871.
(21) Ikeda, J. A. S.; Chiang, Y.-M. Space Charge Segregation at Grain Boundaries in Titanium Dioxide: I. Relationship Between Lattice Defect Chemistry and Space Charge Potential. *J. Am. Ceram. Soc.* **1993**, *76*, 2437−2446.
(22) Ikeda, J. A. S.; Chiang, Y.-M. Space Charge Segregation at Grain Boundaries in Titanium Dioxide: II. Model Experiment. *J. Am. Ceram. Soc.* **1993**, *76*, 2447−2459.
(23) Moulder, J. F.; Stickle, W. F.; Scobol, P. E.; Bomben, K. D. In *Handbook of X-ray Photoelectron Spectroscopy*; Chastain, J., Ed.; Perkin-Elmer Corporation, Physical Electronics Division: Eden Prairie, MN, 1992.
(24) Gao, Y.; Thevuthasan, S.; McCready, D. E.; Engelhard, M. MOCVD Growth and Structure of Nb- and V-Doped TiO_2 Films on Sapphire. *J. Cryst. Growth* **2000**, *212*, 178−190.
(25) Gong, B.; Luo, X.; Bao, N.; Ding, J.; Li, S.; Yi, J. XPS Study of Cobalt Doped TiO_2 Films Prepared by Pulsed Laser Deposition. *Surf. Interface Anal.* **2014**, DOI: 10.1002/sia.5397.
(26) Sham, T. K.; Lazarus, M. S. X-ray Photoelectron Spectroscopy (XPS) Studies of Clean and Hydrated TiO_2 (Rutile) Surfaces. *Chem. Phys. Lett.* **1979**, *68*, 426−432.
(27) Sheppard, L. R.; Bak, T.; Nowotny, J. Electrical Properties of Niobium-Doped Titanium Dioxide. 2. Equilibration Kinetics. *J. Phys. Chem. C* **2006**, *110*, 22455−22461.
(28) Kröger, F. A. *The Chemistry of Imperfect Crystals*; New Holland: Amsterdam, The Netherlands, 1974; Vol. 3, p 275.
(29) Nowotny, M. K.; Bak, T.; Nowotny, J. Electrical Properties and Defect Chemistry of TiO_2 Single Crystal. IV. Prolonged Oxidation Kinetics and Chemical Diffusion. *J. Phys. Chem. B* **2006**, *110*, 16302−16308.